Methods and objects of chemical analysis, 2025, Vol. 20, No. 2, 128–134

Innovative Design and Fabrication of Monolithic Columns Inside Microchip Devices for Determination of Ni(II) Ions

Salam Mohammed Nasser†, Ahmed Ali Alkarimi†*, and Dakhil Nassir Tah‡

† Department of Chemistry, College of Science, University of Babylon, Babylon, 51001 Iraq;
*e-mail: sci.ahmed.ali@uobabylon.edu.iq
‡ Al-Mustaqbal University ,Babylon, 51001, Iraq

Received: February 02, 2025; Accepted: April 28, 2025
DOI: 10.17721/moca.2025.128-134

An innovative system was developed by fabricating a polymer-based monolith as an effective cation-exchange column within a glass microchip, achieved through in situ polymerization of glycidyl methacrylate (GMA), acrylic acid (AAc), and acrylamide (AAm) via free radical polymerization. Epoxy rings on the monolith surface were subsequently sulfonated with Na_2SO_3 at 70°C to form (R-SO_3Na) groups. The microchip was integrated with a modified HPLC system equipped with a 3-way sub-valve (25 µL), allowing for the reagent-injection of the imidazole-azo ligand MPDADPI to react with Ni(II) ions and form a colored complex at 513 nm within 30 seconds. The calibration curve followed Beer's law over the range of 0.001–3.5 µg mL^{-1} (R^2 = 0.9977). Limits of detection (LOD) and quantification (LOQ) were 0.87 and 2.87 ng mL^{-1}, respectively. The method was validated using atomic absorption spectrophotometry (AAS).

Keywords: monolith, in-situ polymerization, microchip device, determination, Ni(II)

Introduction

Metallic nickel is naturally present in the Earth's crust, along with various soluble and insoluble nickel compounds, including sulfides and silicates, which are found in soil [1]. Dietary intake and occupational exposure can lead to the accumulation of significant levels of nickel in various forms within the human body over a lifetime [2]. Despite this, nickel is not considered an essential trace element for humans. Although the levels of nickel components in foods and beverages are generally considered safe for consumption, individuals with a nickel contact allergy, who are at risk of systemic reactions upon ingestion, should limit their dietary exposure [3]. The removal of heavy metals from wastewater is increasingly being achieved through methods such as chemical precipitation, ion exchange, and the use of functionalized polymers, among other technologies [4, 5].

The term "monolith" was initially employed in 1993 to denote a singular functional unit of cellulose sponge utilized for protein separation [6]. Similarly, the designation "monolithic" rapidly gained prevalence to describe large, porous polymers produced through bulk polymerization within a closed mold [7]. Monoliths have diverse applications, including microfluidics [8], gas chromatography (GC) [9], catalysis [10], supported organic processes [11], and solid-phase extraction [12]. Consequently, substantial molecular polymers were developed in the late 1950s for the production of ion-exchange resins with enhanced osmotic shock resistance and accelerated kinetics [13, 14]. Additionally, glycidyl methacrylate (GMA) polymers, a category of reactive resins, have been discovered and have attracted significant interest [15]. The presence of epoxy groups allows for numerous modifications [15]. Various techniques can be employed to modify cross-linked GMA polymers. The resulting polymers have been applied in ion-exchange resins, catalyst supports, enzyme immobilization, and chromatographic separation media [16].

In chiral chromatography, cross-linked polymers derived from glycidyl and hydroxyethyl methacrylate have been demonstrated to be effective support materials [14, 18, 19]. Polymeric monoliths serve various purposes, including applications based on ion exchange [16, 17]. Ion-exchange chromatography is a widely utilized technique for the separation and purification of materials containing charged biomolecules [20]. A key advantage of monolithic chromatography is its high flow rate, which facilitates faster separation. It is comparatively easy to build, has great permeability, quick mass delivery, and high efficiency compared to conventional packed bed columns. This characteristic renders it particularly suitable for large-scale purification and bioprocessing applications, where expedited separation can lead to substantial cost and time efficiencies [21]. Monolithic chromatography offers numerous benefits over traditional chromatographic methods, establishing it as a viable tool for diverse applications. Its high flow rate and capacity to retain a wide range of molecules make it ideal for bioprocessing and other applications necessitating rapid and efficient separation. As research and development efforts continue to advance the field of monolithic chromatography, we anticipate the emergence of even more diverse and innovative applications in the future [22].

Many analytical methods are used for the determination of Ni(II) ions. Ersöz et al. used solid-phase extraction (SPE) columns filled with materials

based on molecularly imprinted polymers (MIPs) to accomplish the most significant of these. Ni had a detection limit of 0.3 ng/mL and concentrations ranging from 0.3 to 25 ng mL^{-1} [23], while Yang et al. discovered that concentrations ranged from 0.005–0.3 mol L^{-1} at a flow rate of 5 mL min^{-1} using rapid column high-performance liquid chromatography (HPLC) [24]; using online and ICP-MS, Suo et al. discovered that Ni concentrations ranged from 0.5 to 100 μg L^{-1}, with a detection limit of 14.7 ng L^{-1} [25]. Chen et al. employed microwave digestion and RP-HPLC followed by on-line column enrichment (OLE) to determine the linear concentration range of 0.01–120 μg L^{-1} Ni and the limit of detection (LOD) of 3.5 ng L^{-1} [26].

In contrast to earlier approaches, our method uses an online FIA-HPLC microchip to measure nickel in wastewater using extremely modest volumes of isocratic elution (pH = 8) for Ni(II). Glass is used as a core material for microchips because of its many qualities, including its great mechanical stability, superb optical transparency, impermeability, chemical inertness, and ability to neither damage nor leak the active ingredients [27]. Glass is a material that is less concerning than polymers because of its chemical compatibility—that is, it is not affected by chemicals. Additionally, it is resistant to harsh cleaning, allowing for repeated use in situations where polymers are typically one-time-use materials. Not all disposables are the most cost-effective or environmentally friendly choice [28]. Glass has a substantially higher stability than polymers. Moreover, glass is resistant to organic solvents and can withstand higher pressures and temperatures [29].

This study aims to develop monolithic columns within microchip devices for the separation and quantification of Ni(II) ions, as well as the removal of nickel ions from aqueous solutions. This study is likely to be of interest to both polymer and analytical chemists, as it integrates chromatography with flow injection and microfluidic injection techniques.

The work presents a novel and innovative system, achieved by preparing a polymer-based monolith for effective cation-exchange column chromatography within a glass microchip by in situ polymerization via a free radical polymerization process. The microchip was interfaced with an HPLC system, which was modified with a three-way sub-valve installed post-monolith microchip to facilitate the injection of the imidazole-azo ligand reagent solution. In addition, this study achieved high precision and rapid estimation of Ni(II) ions within only 30 seconds using cation-exchange column chromatography within a glass microchip, as evidenced by our findings.

Experimental part

Apparatus

Magnetic stirrer/heater (Heidolph RM Hei-Standard, Germany), intelligent HPLC pump (Jasco PU-980, Japan), syringe infusion pump (Kd Scientific, Holliston, MA, USA), ultrasonic bath (India), analytical balance (Denver Instruments TP-214, Germany), double-beam UV–Vis spectrophotometer (Shimadzu UV-1700, Japan), and atomic absorption spectrophotometer (Shimadzu AA-6300, Japan).

Chemicals

All chemicals used in this study were of high purity and obtained from Sigma-Aldrich (USA), unless otherwise specified. The following reagents were employed: glycidyl methacrylate (GMA, 98%), acrylic acid (AAc, 98%), acrylamide (AAm, 98%), ethylene dimethacrylate (EDMA, 98%), 2,2-dimethoxy-2-phenylacetophenone (DAP, 99%), and trimethoxysilyl propyl methacrylate (99%). Solvents included HPLC-grade acetone, hexanol, and ethanol. Additional reagents used were sodium hydroxide (NaOH), hydrochloric acid (HCl), deionized water, and nickel nitrate $Ni(NO_2)3$.

Fabrication of the Microchip for Monolith Integration

A glass microchip composed of two thermally bonded layers was used for the fabrication of monoliths. Each layer was 3 mm thick, resulting in a total chip thickness of 6 mm. The overall dimensions of the chip were 50 mm in length and 15 mm in width. Two inlet/outlet holes (1.5 mm in diameter) were drilled into the top layer using conventional glass drilling techniques to allow the flow of the mobile phase. The bottom layer featured a CNC-milled microchannel with dimensions of 30 mm (length), 1 mm (width), and 50 μm (depth). The final chip structure is illustrated in Figure 1.

Surface Preparation of the Microchip (Silanization)

To ensure firm anchoring of the monolith under high flow conditions, the inner surface of the microchannel was functionalized via a silanization process [30]. Initially, the channel was sequentially rinsed with acetone and deionized water. Surface activation was then performed by treating the channel with 0.2 M sodium hydroxide solution for 1 hour, followed by rinsing with water. Subsequently, the surface was conditioned with 0.2 M hydrochloric acid solution for 1 hour and again thoroughly rinsed with deionized water. The channel was then flushed with ethanol and silanized using a 20% (v/v) solution of 3-(trimethoxysilyl)propyl methacrylate in ethanol. Finally, the chip was dried under a stream of nitrogen gas, rendering it ready for in situ polymerization

Polymerization Process [32]

The monolithic polymer (GMA-co-AAc-co-AAm) was prepared via in situ free-radical polymerization. The polymerization mixture was composed of glycidyl methacrylate (GMA, 500 μL), acrylic acid (AAc, 300 μL), acrylamide (AAm, 400 μL), and ethylene dimethacrylate (EDMA, 60 μL) as the cross-linking agent. The initiator, 2,2-dimethoxy-2-phenylacetophenone (1 wt% relative to the total monomer content), was added to initiate polymerization. A porogenic solvent system consisting of hexanol (650 μL) and ethanol (1000 μL) was used to dissolve all components and to induce the formation of a porous structure. The mixture was purged with

nitrogen gas for 5 minutes to remove dissolved oxygen, then immediately introduced into the microchannel. After sealing the inlet and outlet ports, UV-initiated polymerization was carried out at 365 nm for 1 minute. Following polymerization, the monolith was flushed sequentially with deionized water and absolute ethanol to remove unreacted monomers and porogenic solvents.

Preparation of the Strong Cation-Exchanger Monolithic Column [32, 33]

To convert the reactive epoxy groups on the surface of the (GMA-co-AAc-co-AAm) monolith into strong cation-exchange sites, the monolith was functionalized with a sodium sulfite (Na_2SO_3) solution. A 10 μg/mL Na_2SO_3 solution was pumped through the microchip channel at a flow rate of 30 μL/min for 1 hour at a controlled temperature of 60–75 °C, resulting in the formation of $–SO_3Na$ groups on the polymer surface. Following functionalization, the monolithic column was activated by flushing with 0.2 M HCl, then thoroughly rinsed with deionized water for 1 hour to remove residual reagents and stabilize the surface for subsequent analytical use.

Calibration Curve

A calibration curve for Ni(II) was established over the concentration range of 0.001 to 3.5 μg mL^{-1}. Each concentration point was measured in triplicate to ensure accuracy and reproducibility. Analytical parameters, including linear regression, coefficient of determination (R^2), and standard deviations, were calculated using Microsoft Excel and SPSS version 15 software.

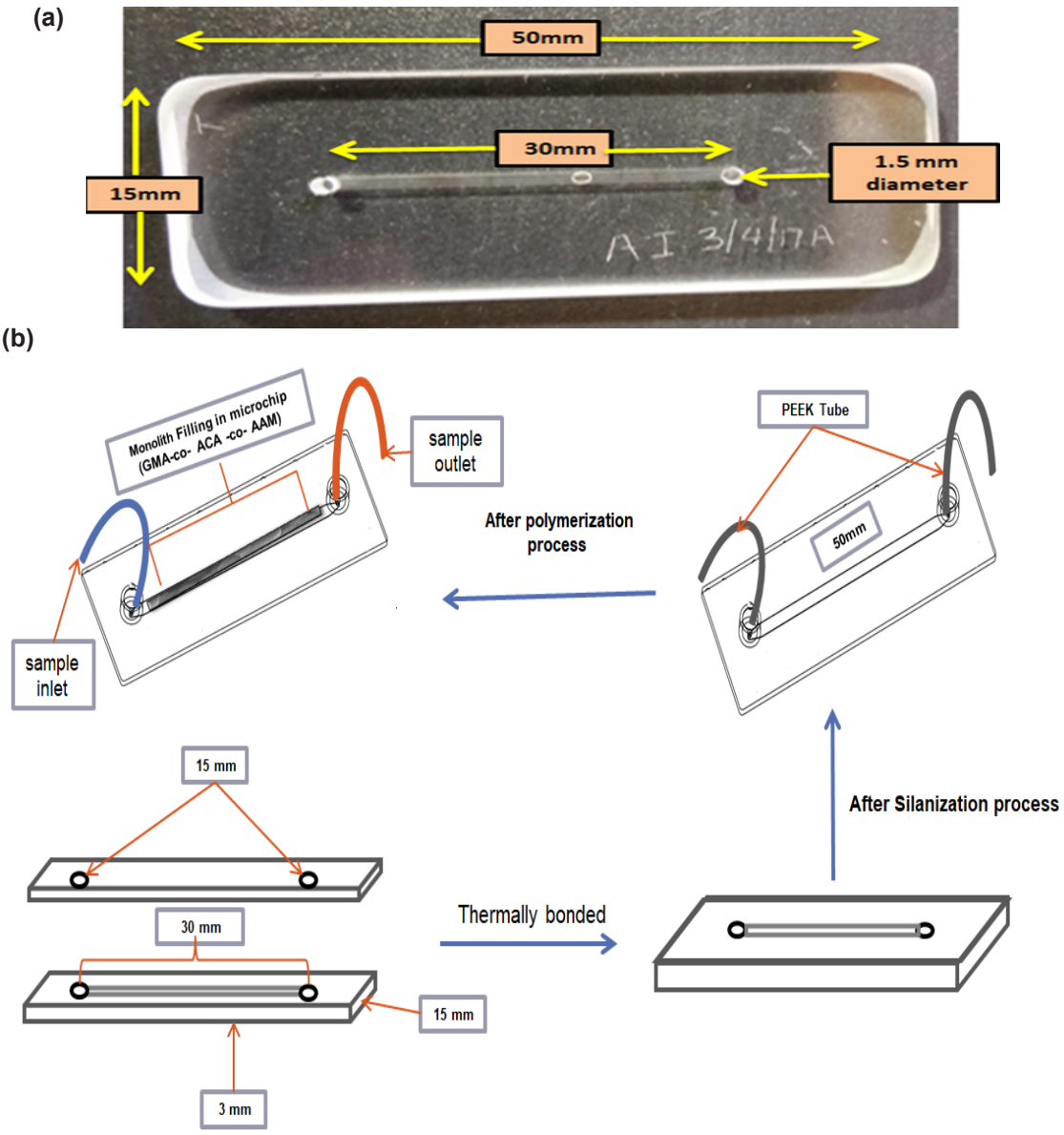

Figure 1. Photograph of the glass microchip used for the separation of Ni(II) ions (a) and schematic stages of designing the microfluidic chip (b).

Results and discussion

Innovative design of the system

The analytical system was designed by integrating an HPLC pump, a manual injector, the fabricated microchip, and a three-way sub-valve to enable the determination of Ni(II) ions. The configuration and operation of the system are illustrated in Figures S1–3.

Firstly, deionized water was pumped through the entire system to wash and remove any substances that could interfere with the sample. After that, Ni(II) (1.5 μg/mL) at 0.5 mL/min was injected in one valve (universal valve) manually using an HPLC needle (250 μL Restek, USA) into the sample loop (100 μL) in two steps: the first step is called "loading sample" at load position (No. 4 position to No. 1 position), and the waste comes out of position No.6, and the second step pushes the sample toward the microchip as shown in Figures 1a, b, and c.

Secondly, when the sample travels through the system, it will pass through the microchip that has the monolith that was prepared by in situ polymerization for Ni determination.

Thirdly, the removal process: when the Ni(II) ions interact with the active groups (-SO_2Na) on the monolith surface, these ions are removed by pumping 0.1 mol/L HCl to remove Ni(II) ions and activate the monolith surface.

Finally, when HCl removes Ni (II) ions, the eluent solution will interact with the reagent solution imidazole-azo ligand (E)-2-(4-methoxyphenol) diazenyl)-4, 5-diphenyl-1Himidazole (MPDADPI) that was prepared and characterized by Naser et al. (35) at the sub-valve (3-way) tied (25 μL) that was installed after the monolith microchip, the reaction time was only (30 seconds) to form a color complex, as shown in Figures 2 a, b, and c. After that, the colored complex was moved towards the detector to draw the signal at 513 nm.

Polymer Formation Inside the Microchip

The successful formation of the monolithic structure inside the microchip was visually confirmed by the appearance of a solid white phase within the microchannel. The (GMA-co-AAc-co-AAm) monolith was synthesized and previously characterized by Nasser et al. [5]. The FTIR spectrum of the unmodified monolith is presented in Figure S4, while the spectrum after sulfonation is shown in Figure S5. The disappearance of the characteristic epoxy group absorption band at 906.14 cm^{-1} indicated successful ring opening of the glycidyl methacrylate units. Two new absorption bands emerged at 1016.06 cm^{-1} and 951.62 cm^{-1}, corresponding to the symmetric stretching of –SO_3^- and S–O bonds, respectively, confirming sulfonation. Additionally, a medium-intensity N–H stretching vibration, characteristic of secondary amines, was observed in the range of 3342.49–3199.65 cm^{-1}. The peaks at 1160.89 cm^{-1} (C–O esters) and 1721.60 cm^{-1} (C=O carbonyl groups) remained unchanged, indicating that these functional groups were not involved in the sulfonation reaction.

The morphology of the synthesized monolith was examined using scanning electron microscopy (SEM). As shown in Figure 2, the monolith exhibits a highly porous structure composed of a network of interconnected channels, which facilitates efficient fluid flow. The presence of macropores (>50 nm) enables rapid transport of the mobile phase through the monolithic matrix, thereby enhancing permeability and minimizing back pressure. In addition to macropores, the monolith contains a distribution of mesopores (2–50 nm), which play a vital role in increasing the surface area and improving the loading capacity of the column. These structural characteristics are essential for the effective performance of the monolith in separation applications. Figure S6 illustrates the monolith formed within the microchip channel.

Permeability

The permeability of the monolithic microchip column was evaluated by monitoring the backpressure generated at various flow rates using an HPLC pump. The relationship between flow rate and pressure was used to assess the flow characteristics and mechanical stability of the monolith. The results, presented in Table S1 and illustrated in Figure S7, demonstrate consistent performance across the tested flow range, indicating the suitability of the monolith for microfluidic applications.

Calibration Curve

A calibration curve for Ni(II) was constructed over the concentration range of 0.001 to 3.5 μg mL^{-1}. The calibration plot is presented in Figure S8. The resulting calibration curve exhibited excellent linearity, with a coefficient of determination (R^2) of 0.9977. The limit of detection (LOD), calculated at a signal-to-noise ratio (S/N) of 3, was 0.87 ng mL^{-1}, while the limit of quantification (LOQ), based on an S/N of 10, was determined to be 2.87 ng mL^{-1}.

Precision and Accuracy

The analytical performance of the monolithic microchip system was evaluated by analyzing standard solutions of Ni(II) at various concentrations (n = 3 for each level). The results demonstrated excellent precision, accuracy, and recovery, confirming the reliability of the developed method. A comparison was made with results obtained using atomic absorption spectrophotometry (AAS), showing strong agreement between the two techniques. Detailed values for standard deviation (S.D.), relative standard deviation (RSD%), recovery, and concentrations found using both methods are presented in Table 1.

Conclusions

In this study, an innovative microfluidic analytical system was successfully developed by integrating a strong cation-exchange monolithic column (GMA-co-AAc-co-AAm) into a glass microchip. The monolith was synthesized via in situ UV-initiated free-radical polymerization, followed by chemical modification

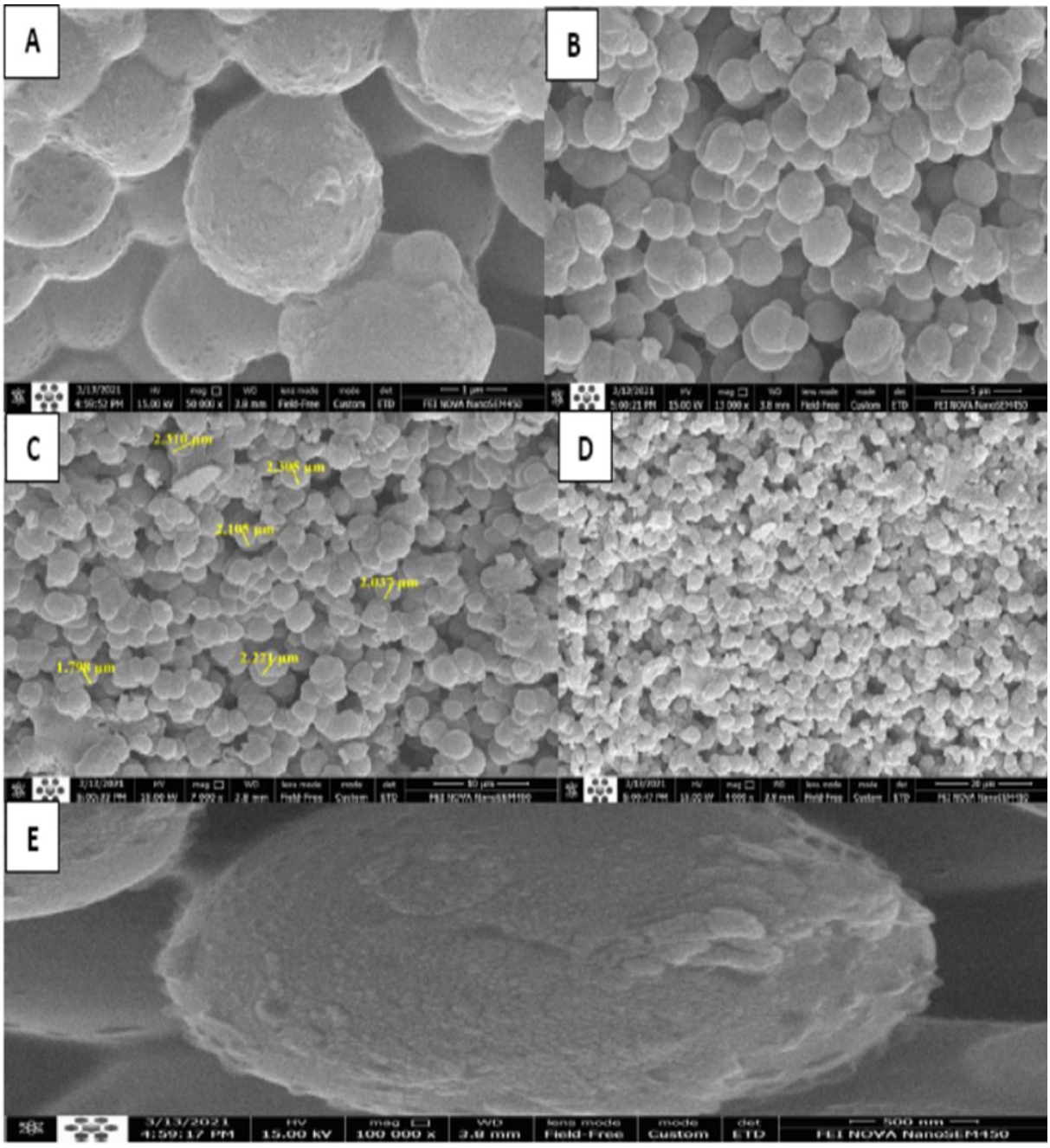

Figure 2. SEM images of monoliths with scale bars of (A) 1 µm, (B) 5 µm, (C) 10 µm, (D) 20 µm, and (E) 500 nm.

Table 1. Comparison of Ni(II) Determination by the Innovative Method and Atomic Absorption Spectrophotometry (AAS).

Conc. of Ni(II) µg mL^{-1}	S.D (n=3)	RSD% (n=3)	Found Con. mg mL^{-1} Using the Innovative method	Recovery (%)	Found Con. µg. mL^{-1} Using an AAS
0.5	0.001	1.657	0.51	102.04	0.50
1	0.001	0.81	0.91	98.21	0.98
1.5	0.003	1.376	1.52	101.68	1.51
2	0.005	1.621	2.01	99.50	2.10
2.5	0.003	0.735	2.50	100.00	2.50
3	0.006	1.316	2.98	100.67	2.92
3.5	0.021	1.220	3.48	99.29	3.49

of the epoxy groups to introduce sulfonic acid functionalities ($–SO_3Na$), enabling selective cation exchange. The resulting device was coupled with a modified HPLC system, incorporating a three-way sub-valve for reagent mixing and online complexation with an imidazole-azo ligand (MPDADPI), facilitating rapid colorimetric detection of Ni(II) ions.

The system demonstrated excellent analytical performance, including high precision, linearity (R^2 = 0.9977), low limits of detection (LOD = 0.87 ng mL^{-1}) and quantification (LOQ = 2.87 ng mL^{-1}), and strong agreement with standard atomic absorption spectrophotometry (AAS). The methodology allowed for the determination of Ni(II) within 30 seconds using minimal reagent and sample volumes, highlighting its potential for high-throughput or field-deployable analysis.

Additionally, the use of glass microchips provides notable advantages over conventional polymer-based devices due to superior chemical resistance, optical transparency, reusability, and pressure tolerance. The system's environmentally friendly profile—owing to its low waste generation, reduced chemical consumption, and compact design—aligns with the principles of green analytical chemistry.

This platform opens new avenues for developing integrated microfluidic devices for trace metal analysis and can be further adapted for the selective detection of other environmentally or biologically relevant metal ions by modifying the monolithic phase or complexing ligands. Future work may focus on automation, multiplexed detection, and integration with portable detection systems for on-site applications.

References

1. Mustafa, A.; Zulfiqar, U.; Mumtaz, M. Z.; Radziemska, M.; Haider, F. U.; Holatko, J.; Brtnicky, M. Nickel (Ni) Phytotoxicity and Detoxification Mechanisms: A Review. *Chemosphere* **2023**, *328*, 138574. https://doi.org/10.1016/j.chemosphere.2023.138574.

2. Mehri, A. Trace Elements in Human Nutrition (II)–An Update. *Int. J. Prev. Med.* **2020**, *11*(1), 2. https://doi.org/10.4103/ijpvm.IJPVM_48_19.

3. Zhao, J.; Shi, X.; Castranova, V.; Ding, M. Occupational Toxicology of Nickel and Nickel Compounds. *J. Environ. Pathol. Toxicol. Oncol.* **2009**, *28*(3). https://doi.org/10.1615/JEnvironPatholToxicolOncol.v28.i3.10.

4. Tamahkar, E.; Bakhshpour, M.; Andaç, M.; Denizli, A. Ion Imprinted Cryogels for Selective Removal of Ni(II) Ions from Aqueous Solutions. *Sep. Purif. Technol.* **2017**, *179*, 36–44. https://doi.org/10.1016/j.seppur.2016.12.048.

5. Nasser, S. M.; Alkarimi, A. A.; Taha, D. N. Preparation and Application of (GMA-co-ACA co-AAM) as Cation-Exchange Monolithic Column for Determination of Nickel (II) Ion. *J. Pharm. Negat. Results* **2022**, *13*(2), 92. https://doi.org/10.47750/pnr.2022.13.02.014.

6. Prakash, S.; Somiya, G.; Elavarasan, N.; et al. Synthesis and Characterization of Novel Bioactive Azo Compounds Fused with Benzothiazole and Their Versatile Biological Applications. *J. Mol. Struct.* **2021**, *1224*, 129016. https://doi.org/10.1016/j.molstruc.2020.129016.

7. Ahmad, S.; Jalagat, R. C.; Alulis, I.; Aquino, P. G. Benchmarking for Competitive Advantage and Organizational Performance: Proposed Framework. *Vidyabharati Int. Interdiscip. Res. J.* **2021**, *12*(1), 67–77.

8. Evard, H.; Priks, H.; Saar, I.; et al. A New Direction in Microfluidics: Printed Porous Materials. *Micromachines* **2021**, *12*(6), 671. https://doi.org/10.3390/mi12060671.

9. Nguyen, V. T.; Nguyen, D. B.; Mok, Y. S.; et al. Removal of Ethyl Acetate in Air by Using Different Types of Corona Discharges Generated in a Honeycomb Monolith Structure Coated with Pd/γ-Alumina. *J. Hazard. Mater.* **2021**, *416*. https://doi.org/10.1016/j.jhazmat.2021.126162.

10. Poupart, R.; Guerrouache, M.; Grande, D.; et al. Gold Nanoparticles Supported onto Amine-Functionalized In-Capillary Monoliths Meant for Flow-Through Catalysis: A Comparative Study. *Polymer* **2021**, *230*, 124014. https://doi.org/10.1016/j.polymer.2021.124014.

11. Arqueros, C.; Zamora, F.; Montoro, C. A Perspective on the Application of Covalent Organic Frameworks for Detection and Water Treatment. *Nanomaterials* **2021**, *11*(7), 1651. https://doi.org/10.3390/nano11071651.

12. Ferrance, J. P. Solid Phase Extraction on Reverse Phase Chromatographic Media Subjected to Stresses Expected for Extraterrestrial Implementation. *Analyst* **2022**, *147*(15), 3514–3524. https://doi.org/10.1039/D2AN00768A.

13. Scorza, L. C.; Simon, U.; Wear, M.; et al. Evaluation of Novel 3D-Printed Monolithic Adsorbers Against Conventional Chromatography Columns for the Purification of C-Phycocyanin from Spirulina. *Algal Res.* **2021**, *55*, 102253. https://doi.org/10.1016/j.algal.2021.102253.

14. Simon, U.; Scorza, L. C.; Teworte, S.; et al. Demonstration of Protein Capture and Separation Using Three-Dimensional Printed Anion Exchange Monoliths Fabricated in One-Step. *J. Sep. Sci.* **2021**, *44*(6), 1078–1088. https://doi.org/10.1002/jssc.202000722.

15. Wale, A.; Mulani, K.; Deshpande, S.; et al. Construction of β-Cyclodextrin Linked Glycidyl Methacrylate Polymers for Stereoselective Separation of Chiral Drug. *J. Polym. Res.* **2021**, *28*, 1–13. https://doi.org/10.1007/s10965-021-02634-7.

16. Araya-Farias, M.; Dziomba, S.; Tran, N. T. Microfluidic Strategies for Extraction and Preconcentration of Proteins and Peptides. In *Handbook on Miniaturization in Analytical Chemistry*; Elsevier:

Amsterdam, 2020; pp 35–75. https://doi.org/10.1016/B978-0-12-819763-9.00003-9.

17. Abed, E. F.; Alkarimi, A. A. Ion Exchange Monolithic Column for Copper Determination. *Acta Chem. Iasi* **2021**, *29*(2), 151–165. https://doi.org/10.47743/achi-2021-2-0011.

18. Hutchinson, J. P.; Zakaria, P.; Bowie, A. R.; et al. Latex-Coated Polymeric Monolithic Ion-Exchange Stationary Phases. 1. Anion-Exchange Capillary Electrochromatography and In-Line Sample Preconcentration in Capillary Electrophoresis. *Anal. Chem.* **2005**, *77*(2), 407–416. https://doi.org/10.1021/ac048748d.

19. Alkarimi, A. A.; Welham, K. Proteins Pre-Concentration Using Glycidyl Methacrylate-co-Stearyl Methacrylate-co-Ethylene Glycol Dimethacrylate Monolith. *Indones. J. Chem.* **2020**, *20*(5), 1143–1151. https://doi.org/10.22146/ijc.49479.

20. Khalaf, I. A. H.; Alkarimi, A. A. Bovine Serum Albumin Pre-Concentration Using Glycidyl Methacrylate-co-Ethylene Glycol Dimethacrylate-co-(2-Diethylamino) Ethyl Methacrylate Monolith. *Egypt. J. Chem.* **2021**, *64*(9), 5137–5141. https://doi.org/10.21608/ejchem.2021.68171.3485.

21. Guiochon, G. Monolithic Columns in High-Performance Liquid Chromatography. *J. Chromatogr. A* **2007**, *1168*(1–2), 101–168. https://doi.org/10.1016/j.chroma.2007.05.090.

22. Souza, I. D.; Queiroz, M. E. C. Organic-Silica Hybrid Monolithic Sorbents for Sample Preparation Techniques: A Review on Advances in Synthesis, Characterization, and Applications. *J. Chromatogr. A* **2024**, *1713*, 464518. https://doi.org/10.1016/j.chroma.2023.464518.

23. Ersöz, A.; Say, R.; Denizli, A. Ni(II) Ion-Imprinted Solid-Phase Extraction and Preconcentration in Aqueous Solutions by Packed-Bed Columns. *Anal. Chim. Acta* **2004**, *502*(1), 91–97. https://doi.org/10.1016/j.aca.2003.09.059.

24. Yang, G.; Hu, Q.; Huang, Z.; Yin, J. Determination of Pb, Cd, Hg, Ni and Zn by a Rapid Column High-Performance Liquid Chromatography. *J. Braz. Chem. Soc.* **2005**, *16*, 1154–1159. https://doi.org/10.1021/ac00132a005.

25. Suo, F.; Chen, B.; He, M.; Hu, B. Monolithic Capillary Microextraction On-Line Combined with ICP-MS for Determining Ni, Cu and Cd in Biological Samples. *Anal. Methods* **2016**, *8*(23), 4680–4688. https://doi.org/10.1039/C6AY01008C.

26. Chen, Z.; Yang, G. Y.; Wang, S.; et al. Simultaneous Determination of Tin, Nickel, Lead, Cadmium and Mercury in Tobacco and Tobacco Additives by Microwave Digestion and RP-HPLC Followed by On-Line Column Enrichment. *J. Chin. Chem. Soc.* **2004**, *51*(1), 71–77. https://doi.org/10.1002/jccs.200400012.

27. Lauge-Kristensen, R.; Best, R. Future Technologies: New Materials and Techniques. In *Design and Construction*; Routledge: London, 2007; pp 418–434.

28. Jalil, M. A.; Halim, A. F.; Moniruzzaman, M.; et al. Nanomaterials in Textile Processing. In *Adv. Technol. Text.* Springer Nature: Singapore, 2023; pp 323–344. https://doi.org/10.1002/adma.201802822.

29. Varley, R. J.; Leong, K. H. Polymer Coatings for Oilfield Pipelines. In *Active Protective Coatings: New-Generation Coatings for Metals*; Springer: Dordrecht, 2016; pp 385–428. https://doi.org/10.1007/978-94-017-7540-3_14.

30. Poddar, S.; Sharmeen, S.; Hage, D. S. Affinity Monolith Chromatography: A Review of General Principles and Recent Developments. *Electrophoresis* **2021**, *42*(24), 2577–2598. https://doi.org/10.1002/elps.202100163.

31. Shareef, Z. H.; Alkarimi, A. A. Estimation for Warfarin in Pharmaceutical Preparation Using Monolithic Column. *Anal. Sci. Technol.* **2024**, *37*(4), 220–229. https://doi.org/10.5806/AST.2024.37.4.220.

32. Naser, S. M. Optimization and Modelling of Electrochemical Removal of Nitrate from Solutions. In *Curr. Trends Geotech. Eng. Constr.*, Springer: Singapore, 2022; Vol. 62. https://doi.org/10.1007/978-981-19-7358-1_7.

33. Paul, S.; Rånby, B. MMA-GMA Copolymers: A Novel Method to Introduce Sulfonic Acid Groups on the Polymeric Chains. *Macromolecules* **1976**, *9*(2), 337–340. https://doi.org/10.1021/ma60050a031.

34. Nasser, S. M.; Alkarimi, A. A.; Taha, D. N. Synthesis of (E)-2-(4-Methoxyphenol) Diazenyl)-4,5-Diphenyl-1H-Imidazole (MPDADPI) for Ni(II) Determination Separated Off-Line Using Monolithic Column. *HIV Nurs.* **2022**, *22*(2), 895–898. https://doi.org/10.31838/hiv22.02.175.